

Single and double Wiebe function combustion model for a heavy-duty diesel engine retrofitted to natural-gas spark-ignition

Jinlong Liu, Cosmin E. Dumitrescu*

Mechanical and Aerospace Engineering, West Virginia University, Morgantown, WV, USA

HIGHLIGHTS

- Two-stage combustion process compared to conventional gasoline engine.
- Standard Wiebe-function predicted badly the mass fraction burned and heat release.
- Double-Wiebe function reduced the error by 90% and captured the two stages.
- A condition-independent model can be developed if enough data for calibration.

ARTICLE INFO

Keywords:

Double-Wiebe function
Two-stage combustion
Natural gas
Spark ignition
Lean burn
Diesel geometry

ABSTRACT

The conversion of existing diesel engines to natural-gas spark-ignition operation would reduce the dependence on oil imports, reduce the burden on refining capacity, and increase U.S. energy security. The use of simple combustion models such as the Wiebe function to analyze or predict the combustion process in such retrofitted engines can accelerate and optimize the engine conversion. This study compared the standard single Wiebe function to a double-Wiebe function to investigate if the latter will improve the predicted mass fraction burned and, if yes, which of formats of the dual-Wiebe function in the literature described the best the mass fraction burned in such converted engine. The results showed that while the standard Wiebe function could not predict the mass fraction, a double-Wiebe function (one for the fast burn inside the piston bowl and a second for the slower burning process inside the squish region) predicted with good accuracy the mass fraction burned, heat release rate, in-cylinder pressure, and combustion phasing in such converted engines (~90% reduction in error) for the conditions investigated here, especially if the start of the second Wiebe was delayed. Moreover, such a condition-dependent model as the double-Wiebe model is limited to the operating conditions used for determining the model parameters. However, the model can be developed into a condition-independent model if enough experimental data or CFD simulations are available to find the unique set (or sets) of parameters that minimizes the error at most conditions.

1. Introduction

The conversion of existing diesel engines to natural-gas (NG) spark-ignition (SI) operation would reduce the dependence on oil imports, reduce the burden on refining capacity, and increase U.S. energy security [1]. These engines can also operate leaner than traditional SI engines (which would increase engine efficiency and reduce emissions) [2] because the conventional diesel combustion chamber (i.e., flat head and bowl-in-piston) is a “fast-burn” chamber [3]. However, the interaction between in-cylinder turbulence, combustion chamber geometry, and chemistry in such engines greatly affects the combustion phenomena compared to the conventional SI combustion [4]. Specifically,

the different flow patterns and turbulence levels during the compression and expansion strokes will produce a different flame propagation scenario [5]. Previous studies reported a strong flow from the squish towards the bowl during the compression stroke [6]. A secondary tumble flow was produced by the interaction between the squish flow and the piston movement [7]. These two major motions increased the turbulence inside the bowl around top-dead-center (TDC) compared to that inside the squish band [8]. It was reported that this flow motion (which is specific to the diesel geometry) partitioned the whole combustion event into two separate processes with respect to their timing and location [9]. The flame was thick but propagated fast inside the bowl region [10]. By comparison, the flame inside the squish volume

* Corresponding author at: West Virginia University, P.O. Box 6106, Morgantown, WV 26506, USA.

E-mail address: cedumitrescu@mail.wvu.edu (C.E. Dumitrescu).

<https://doi.org/10.1016/j.apenergy.2019.04.098>

Received 28 January 2019; Received in revised form 18 March 2019; Accepted 16 April 2019

Available online 23 April 2019

0306-2619/ © 2019 Elsevier Ltd. All rights reserved.

was thinner and propagated much slower [11]. Moreover, while the high turbulence inside the bowl accelerated the turbulent flame speed during the first combustion stage [12], the lower turbulence inside the squish region, the reduction in temperature and pressure during the expansion stroke, and the higher surface/volume ratio greatly reduced the turbulent flame speed [13]. These phenomena can influence engine efficiency and emissions if not well understood [14].

The Wiebe function is a zero-dimensional engine model widely-used in engine development [15], particularly for SI applications [16]. It is a relatively simple way to approximate the mass fraction burned (MFB) during the combustion process compared to more complex combustion models [17]. The standard Wiebe function is expressed as:

$$x_b(\theta) = 1 - \exp\left[-a\left(\frac{\theta - \theta_0}{\Delta\theta}\right)^{m+1}\right] \quad (1)$$

where $x_b(\theta)$ is the mass fraction burned, θ is the crank angle, θ_0 is the crank angle at the start of combustion (SOC), $\Delta\theta$ is the combustion duration defined as the difference between SOC, θ_0 , and the end of combustion (EOC), θ_{EOC} (i.e., $\Delta\theta = \theta_{EOC} - \theta_0$), m is the form factor because it determines the shape of the combustion process curve, and a is the efficiency parameter because it controls the duration of the combustion process. The integral of $x_b(\theta)$ over the whole combustion duration $\Delta\theta$ is close to but never equal to one, as the equality is only possible if a is equal to infinity. The standard Wiebe function in Eq. (1) was shown to predict with good accuracy the MFB in conventional stoichiometric SI engines [3]. However, the standard Wiebe function was less accurate when large variations in the burning rate were present such as those in advanced combustion strategies [15]. To account for these variations, Yasar et al. [15] introduced a 2nd Wiebe function to describe the MFB in a homogeneous charge compression ignition (HCCI) engine. The 2nd Wiebe function was associated just to the slower combustion near the wall. To ensure that the exponential term in each Wiebe function was near zero at the end of each combustion stage, Ref. [15] introduced two more terms, as seen in Eq. (2):

$$x_b(\theta) = \lambda \left\{ 1 - \exp\left[-a\left(\frac{\theta - \theta_0}{\Delta\theta}\right)^{m+1}\right] \right\} + (1 - \lambda) \left\{ 1 - \exp\left[-a\left(\frac{\theta - \theta_0}{k\Delta\theta}\right)^{m+1}\right] \right\} \quad (2)$$

where λ is the fraction of the mixture that burns in the fast combustion stage and k is the ratio of the slow to the fast burn durations. While this approach improved the predictions, similar a and m and θ_0 for both Wiebe function will result in similar burn rates at the start of each stage. Moreover, it assumes that both stages started at the same time, which may not be the case in the real process. Yeliana et al. [16] improved the double-Wiebe function shown in Eq. (2) by combining a and $\Delta\theta$ into one factor α and by allowing α and m to have different values, as seen in Eq. (3):

$$x_b(\theta) = \lambda \left\{ 1 - \exp\left[-\left(\frac{\theta - \theta_0}{\alpha_1}\right)^{m_1+1}\right] \right\} + (1 - \lambda) \left\{ 1 - \exp\left[-\left(\frac{\theta - \theta_0}{\alpha_2}\right)^{m_2+1}\right] \right\} \quad (3)$$

where α_i is the combined factor for the fast ($i = 1$) or the slow ($i = 2$) combustion process. They claimed that their five-parameter model (α_1 , α_2 , m_1 , m_2 , and λ) predicted very well the MFB of a SI engine running on ethanol-gasoline blends at multiple operating conditions, despite their model assuming that both stages started at the same time. Glewen et al. [18] used a double Wiebe function with unique and independent values of a and m , but same $\Delta\theta$ and θ_0 to describe the flame propagation and autoignition that occurred simultaneously in HCCI engines. Tolou et al. [19] improved Eq. (2) when using the double-Wiebe function model to separate the initial rapid premixed-combustion from the gradual,

diffusion-like combustion of the liquid fuel film on the piston or cylinder walls in a homogeneous-charge gasoline direct-injection (GDI) engine. Their double-Wiebe function used six variables (λ , m_1 , m_2 , $\Delta\theta_1$, $\Delta\theta_2$ and θ_0), as shown in Eq. (4):

$$x_b(\theta) = \lambda \left\{ 1 - \exp\left[-a\left(\frac{\theta - \theta_0}{\Delta\theta_1}\right)^{m+1}\right] \right\} + (1 - \lambda) \left\{ 1 - \exp\left[-a\left(\frac{\theta - \theta_0}{\Delta\theta_2}\right)^{m+1}\right] \right\} \quad (4)$$

where $a = -\ln(0.001) = 6.9$ (i.e., it was assumed that the exponential factor will be equal to 0.001 at the end of each combustion stage). Their results showed that the double-Wiebe function model reproduced reasonably well both in-cylinder pressure and heat release in the GDI engine. Other researchers considered the addition of a third Wiebe function to further separate a multi-stage combustion process. For example, Awad et al. [20] used a triple-Wiebe function similar to the one described in Eq. (4) but with different a and θ_0 to simulate all combustion phases when biodiesel was used in a diesel engine. Xu et al. [21,22] applied a triple-Wiebe function to predict the burning process after dividing the NG-diesel double-fuel combustion into four stages (diesel premixed, diesel diffusion, NG volumetric combustion, and NG flame propagation). Caligiuri et al. [23] also used a triple-Wiebe function to describe and predict the heat release rate of a double-fuel engine. Larimi et al. [24] proved that the triple-Wiebe combustion model was effective in predicting the heat release rate with two peaks and a long tail from a double-piston, two-stroke, compression-ignition free-piston engine. However, there are no references in the literature that used a multiple-Wiebe function to describe the lean premixed combustion inside a diesel engine retrofitted to NG SI. As Ref. [14] showed that the squish region in such retrofitted engines contained an important fuel fraction that combusted *after* the fast burn inside the piston bowl, it suggested that the standard Wiebe function will not predict the burning rate correctly. As a result, the goal of this paper was to investigate if a double-Wiebe function (i.e., 1st Wiebe function associated to the fast burn and the 2nd Wiebe function associated to the slower burn inside the squish) will improve the MFB prediction and, if yes, which format of the dual-Wiebe function in existing studies (such as the formats shown in Eqs. (2)–(4)) had the best accuracy for such an engine. Furthermore, it investigated what methodology should be used for finding that unique set of parameters that would accurately describe the MFB in a diesel engine converted to lean NG SI operation (even if engine specific or else), similar to what the original standard Wiebe function proposed.

2. Experimental apparatus

Detailed information about the experimental setup that collected the data used in this work is shown in Ref. [25]. Just the major details are presented here. A single-cylinder research engine (Ricardo/Cussons, U.K., Model Proteus), based on a commercial heavy-duty diesel engine (Volvo, Sweden, Model TD120), produced the experimental data. Engine schematic and specifications are shown in Fig. 1 and Table 1, respectively. The original diesel engine configuration was modified to a spark ignition engine by replacing the main injector with a NG spark plug (Stitt, U.S., Model S-RSGN40XLBEX8.4-2). NG was delivered inside the intake manifold using a low-pressure gas injector (Rail Spa, Italy, Model IG7 Navajo) operated at 35 psi, immediately after the intake valve opened. There were no other modifications to the engine head and the original diesel piston was maintained to reduce the conversion cost.

Experiments used chemically pure methane (99.5 vol%) at lean mixture conditions (equivalence ratio $\phi = 0.73$) and low engine speed (900 rpm). Knock-free operation was obtained with a spark timing of -10 CAD ATDC. The indicated mean effective pressure (IMEP) was 8.2 bar.

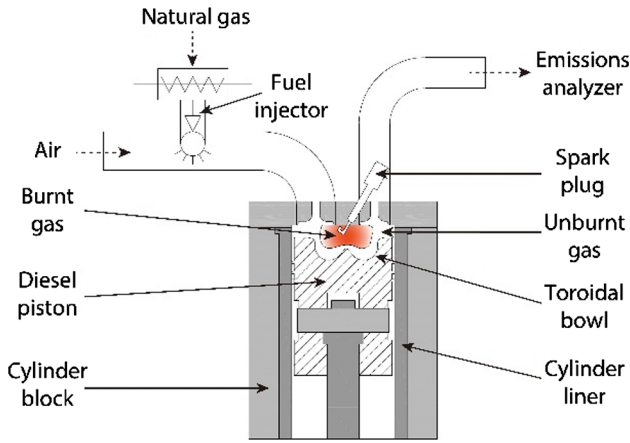


Fig. 1. Schematic of experimental setup.

Table 1
Engine specifications.

Bore × Stroke	130.2 mm × 150 mm
Intake valve opens/closes	12 CAD BTDC/40 CAD ABDC
Exhaust valve opens/closes	54 CAD BBDC/10 CAD ATDC
Connecting rod length	275 mm
Displacement	1.997 L
Compression ratio	13.3
Combustion chamber	Flat head and bowl-in-piston

3. Wiebe-function combustion model

The *Introduction* mentioned that the Wiebe function predicts the MFB versus crank angle, during the combustion process. This section improves the discussion in the *Introduction* by providing additional details about each Wiebe function format described in Eqs. (1)–(4).

3.1. Standard Wiebe function

The start of combustion is a major parameter in the Wiebe function, as seen in Eq. (1). While the location of the first detectable combustion does not coincide with the spark timing (due to the time needed for the flame kernel to develop), θ_0 is usually associated to the spark timing [16]. Moreover, there is no consensus with respect to the combustion duration, $\Delta\theta$. For example, $\Delta\theta$ can be defined as the crank angle interval between 5% MFB (i.e., MFB5) and 95% MFB (i.e., MFB95). The least squares method is usually applied to determine the values of a and m by comparing the Wiebe function to the MFB calculated as the ratio of the cumulative heat release to the total heat release. Moreover, the MFB predicted with the standard Wiebe function has a characteristic S-shape [26].

3.2. Double Wiebe function

The double-Wiebe function assumes that the majority of fuel burns fast but there is a fuel fraction (typically higher than 10%) that burns at a reduced rate. Compared to the standard Wiebe function, the form factor m_i has a wider range of values [15]. While Eq. (2) assumes that the fast- and the slow-burning events start at the same time, the combustion duration may or may not be the same. For simplicity, this work will use the same combustion duration (i.e., $k = 1$ in Eq. (2)), as the different efficiency parameters a_i will compensate for a faster or slower burn duration even if $\Delta\theta$ was the same:

$$x_b(\theta) = \lambda \left\{ 1 - \exp \left[-a_1 \left(\frac{\theta - \theta_0}{\Delta\theta} \right)^{m_1+1} \right] \right\} + (1 - \lambda) \left\{ 1 - \exp \left[-a_2 \left(\frac{\theta - \theta_0}{\Delta\theta} \right)^{m_2+1} \right] \right\} \quad (5)$$

The double-Wiebe function format in Eq. (5) will be referred to as the 1st double -Wiebe format.

If a and $\Delta\theta$ are not combined in the α term, Eq. (3) can be written as:

$$x_b(\theta) = \lambda \left\{ 1 - \exp \left[-a \left(\frac{\theta - \theta_0}{\Delta\theta_1} \right)^{m_1+1} \right] \right\} + (1 - \lambda) \left\{ 1 - \exp \left[-a \left(\frac{\theta - \theta_0}{\Delta\theta_2} \right)^{m_2+1} \right] \right\} \quad (6)$$

where $\Delta\theta_i$ is the combustion duration for the fast ($i = 1$) or the slow ($i = 2$) combustion stages. This study follows the approach shown in [19] by using the same $a = -\ln(0.001) = 6.9$ for both Wiebe functions. Again, this double-Wiebe-function format the fast- and the slow-burning events are assumed to start at the same time. The double-Wiebe function format in Eq. (6) will be referred to as the 2nd double -Wiebe format.

This study proposes two major improvements to Eq. (4). First, the fast and slow burning stages start at different times. In addition, it introduces the signum function to ensure that the calculation uses the 2nd Wiebe function only for crank angles higher than the start of the 2nd combustion stage:

$$x_b(\theta) = \lambda \left\{ 1 - \exp \left[-a_1 \left(\frac{\theta - \theta_{0,1}}{\Delta\theta_1} \right)^{m_1+1} \right] \right\} + (1 - \lambda) \frac{1 + \text{sign}(\theta - \theta_{0,2})}{2} \left\{ 1 - \exp \left[-a_2 \left(\frac{\theta - \theta_{0,2}}{\Delta\theta_2} \right)^{m_2+1} \right] \right\} \quad (7)$$

where $\theta_{0,i}$ is the start of the fast ($i = 1$) or the slow ($i = 2$) combustion processes, and $\text{sign}(\theta - \theta_{0,2})$ equals -1 if $\theta \leq \theta_{0,2}$ and equals 1 if $\theta > \theta_{0,2}$. As a result, $x_b(\theta)$ is associated to the fast-burn if $\theta \leq \theta_{0,1}$, and is associated to both fast- and slow-burn combustion if $\theta > \theta_{0,1}$. Usually, while the choice of $\Delta\theta_i$ may differ from the actual stage duration, the efficiency parameter a_i will correct it towards the real combustion duration. The double-Wiebe function format in Eq. (7) will be referred to as the 3rd double -Wiebe format.

3.3. Model validation

The combustion model used the experimental data to find the set of parameters that will reduce the prediction error of each of the Wiebe function formats. Then, this work assumed that the apparent heat release rate (AHRR) was the derivative of the mass fraction burned per crank angle, as shown in Eq. (8):

$$\frac{dQ_n}{d\theta} = \frac{dx_b(\theta)}{d\theta} m_{fuel} \cdot LHV_{fuel} \cdot \eta_{comb} - \frac{dQ_{ht}}{d\theta} \quad (8)$$

where $(dQ_n)/d\theta$ is the net AHRR, m_{fuel} is the mass of fuel inside the cylinder after intake valve closing, LHV_{fuel} is the lower heating value of the fuel, η_{comb} is the combustion efficiency, and $(dQ_{ht})/d\theta$ is the heat transfer rate during the burning process, calculated using the Woschni equation [27].

The single-zone heat-release model was then used to predict in-cylinder pressure during the combustion process:

$$\frac{dP}{d\theta} = \frac{\gamma - 1}{V} \frac{dQ_n}{d\theta} - \frac{P}{V} \frac{dV}{d\theta} \quad (9)$$

where V is the in-cylinder volume, γ is the specific heat ratio which equals with 1.35 in this work ($\gamma = 1.35$ was assumed to be the average of γ values during the compression and expansion, respectively), and P

is the in-cylinder pressure. Eq. (10) shows the detailed solution of Eq. (9), starting from spark timing:

$$P_{i+1} = P_i + \frac{\frac{\Delta Q_n}{\Delta \theta} - \left(\frac{\gamma}{\gamma-1}\right) \frac{\Delta V}{\Delta \theta} P_i}{\left(\frac{1}{\gamma-1}\right) V} \Delta \theta \quad (10)$$

Consequently, the combustion model was validated by using the fitted Wiebe function to estimate the rate of heat release, then applying this information to predict the cylinder pressure during combustion process. The accuracy of each double-Wiebe function format was evaluated the root-mean-square error (RMSE) to compare the predicted heat release rate and in-cylinder pressure with the experimental data. RMSE was defined as:

$$RMSE = \sqrt{\frac{1}{n} \sum_1^n (y_p - y_E)^2} \quad (11)$$

where y_p and y_E are the predicted and experimental values, respectively, and n is the number of values used for comparison. The sampling frequency used was that of the experimental data (i.e., 0.1 CAD). When estimating the goodness of fit of the model, the better prediction was the one that minimized the RMSE.

4. Results

As the experimental pressure trace was used to determine the Wiebe function parameter, care was taken to ensure a proper conditioning of pressure data. First, the raw pressure was “pegged” to the intake pressure. Next, pressure trace under motoring conditions was used to check for eventual charge leakage through the in-cylinder pressure sensor cables. After ensuring that no charge leakage affected the pressure signal, the raw pressure data was filtered to remove the high-frequency noise. Fig. 2 shows an example of the raw and filtered pressure signal and the corresponding apparent heat release rate.

Four hundred engine cycles were collected and used for the analysis in this work. Fig. 3 compares the heat released during combustion, Q_{ch} with the total fuel chemical energy, $m_f Q_{LHV}$, for the operating conditions investigated in this study. Q_{ch} is the sum of the net (or apparent) heat release, Q_n and the heat loss through the boundaries, Q_{ht} . The difference between the total Q_{ch} and the total fuel chemical energy, $m_f Q_{LHV}$ is due to process inefficiency and blow-by effects. This study used the apparent heat release rate to determine the Wiebe function parameters. In addition, the total combustion duration, $\Delta \theta$, is important

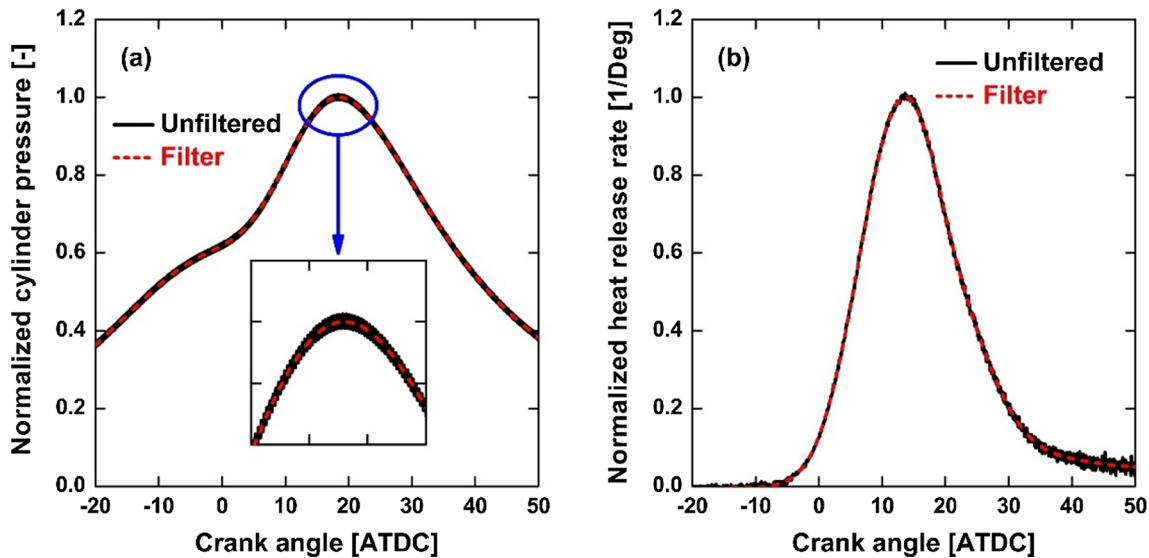


Fig. 2. Unfiltered and filtered in-cylinder pressure trace and the corresponding apparent heat release rate.

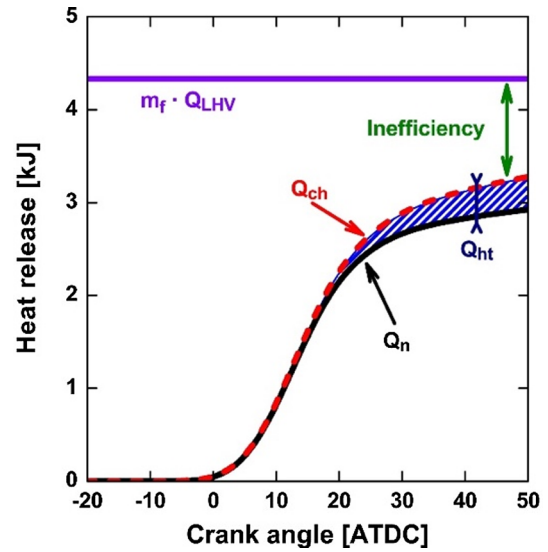


Fig. 3. In-cylinder heat release analysis (Q_n , Q_{ht} , Q_{ch} , m_f and Q_{LHV} are the net (apparent) heat release, the heat loss to the boundaries, the total in-cylinder chemical heat release, in-cylinder fuel mass, and the fuel’ lower heating value, respectively).

for calibrating the Wiebe function. But it is not easy to determine the actual end of combustion because the heat release rates around EOC are comparable to the heat loss to the boundaries. As a result, if CA_x was defined as the crank angle associated with x% of energy-release, EOC in SI combustion is usually defined as CA₉₀ or CA₉₅ based on data such as those presented in Fig. 2. CA₉₀ and CA₉₅ were 28.8 and 54.9 CAD ATDC, respectively, for the conditions investigated here. Consequently, this study started by assuming $\Delta \theta = 50$, which was equivalent to the EOC between CA₉₀ and CA₉₅. Eqs. (12) and (13) show the parameters that minimized the RMSE of the standard and the 1st double-Wiebe function formats, respectively, shown in Eqs. (1) and (5), relative to the experimental data. The RMSE values were based on matching the experimental data from -10 CAD ATDC (spark timing) to 50 CAD ATDC, which was 10 CAD longer than the assumed total combustion duration in the Wiebe function, but still before CA₉₅.

$$x_b(\theta) = 1 - \exp \left[-5.64 \left(\frac{\theta + 10}{50} \right)^{3.73} \right] \quad (12)$$

$$x_b(\theta) = 0.69 \left\{ 1 - \exp \left[-19.68 \left(\frac{\theta + 10}{50} \right)^{3.41} \right] \right\} + 0.31 \left\{ 1 - \exp \left[-2.41 \left(\frac{\theta + 10}{50} \right)^{3.22} \right] \right\} \quad (13)$$

Eq. (14) show the parameters the parameters that minimized the RMSE of the 2nd Wiebe-function format relative to the experimental data, when $a_i = 6.9$:

$$x_b(\theta) = 0.69 \left\{ 1 - \exp \left[-6.9 \left(\frac{\theta + 10}{38.89} \right)^{4.18} \right] \right\} + 0.31 \left\{ 1 - \exp \left[-6.9 \left(\frac{\theta + 10}{69.26} \right)^{3.22} \right] \right\} \quad (14)$$

Eq. (15) show the parameters the parameters that minimized the RMSE of the 3rd Wiebe-function format relative to the experimental data, when the two combustion stages started at different times:

$$x_b(\theta) = 0.73 \left\{ 1 - \exp \left[-5.02 \left(\frac{\theta + 10}{35} \right)^{4.19} \right] \right\} + 0.27 \left[\frac{1 + \text{sign}(\theta - 11)}{2} \right] \left\{ 1 - \exp \left[-2.44 \left(\frac{\theta - 11}{30} \right)^{1.82} \right] \right\} \quad (15)$$

Fig. 4 compares the MFB predicted by the four Wiebe function formats shown in Eqs. (12)–(15) to the mass fraction burned from the experimental data. Fig. 4a shows that the MFB predicted with the standard Wiebe function was far from the experimental data. The results confirmed the initial hypothesis that the standard Wiebe function will not accurately characterize the MFB for the two-stage lean NG SI premixed burning in a bowl-in-piston geometry. For example, Fig. 4a shows that the standard Wiebe predicted a delayed flame propagation inside the bowl then accelerated the late combustion in the squish region. Fig. 4b and c present the MFB predicted by the 1st and 2nd double-Wiebe function formats, which assumed that both the fast- and the slow-burn stages started at the same. The main difference between these two double-Wiebe functions is the variable used for calibration. Specifically, the 1st double-Wiebe format uses the efficiency parameter a to control the duration of combustion, while the 2nd double-Wiebe format uses the combustion stage duration $\Delta\theta$ as a variable, with constant a . The values of the efficiency parameter a in the literature are from 2.3026 and 6.9078, when the combustion duration was defined as the 0–90% or 0–99.9% mass fraction burned, respectively. The range of the form factor m is wider in order to account for faster or slower heat release. For example, a smaller value of m will result in a higher initial mass fraction burned but slower late-burn, while a larger value of m will result in a lower initial mass fraction burned but faster late-burn. A value of $m = 2.5$ will produce a symmetrical mass fraction burn with respect to the median crank angle in $\Delta\theta$, hence its use in the standard

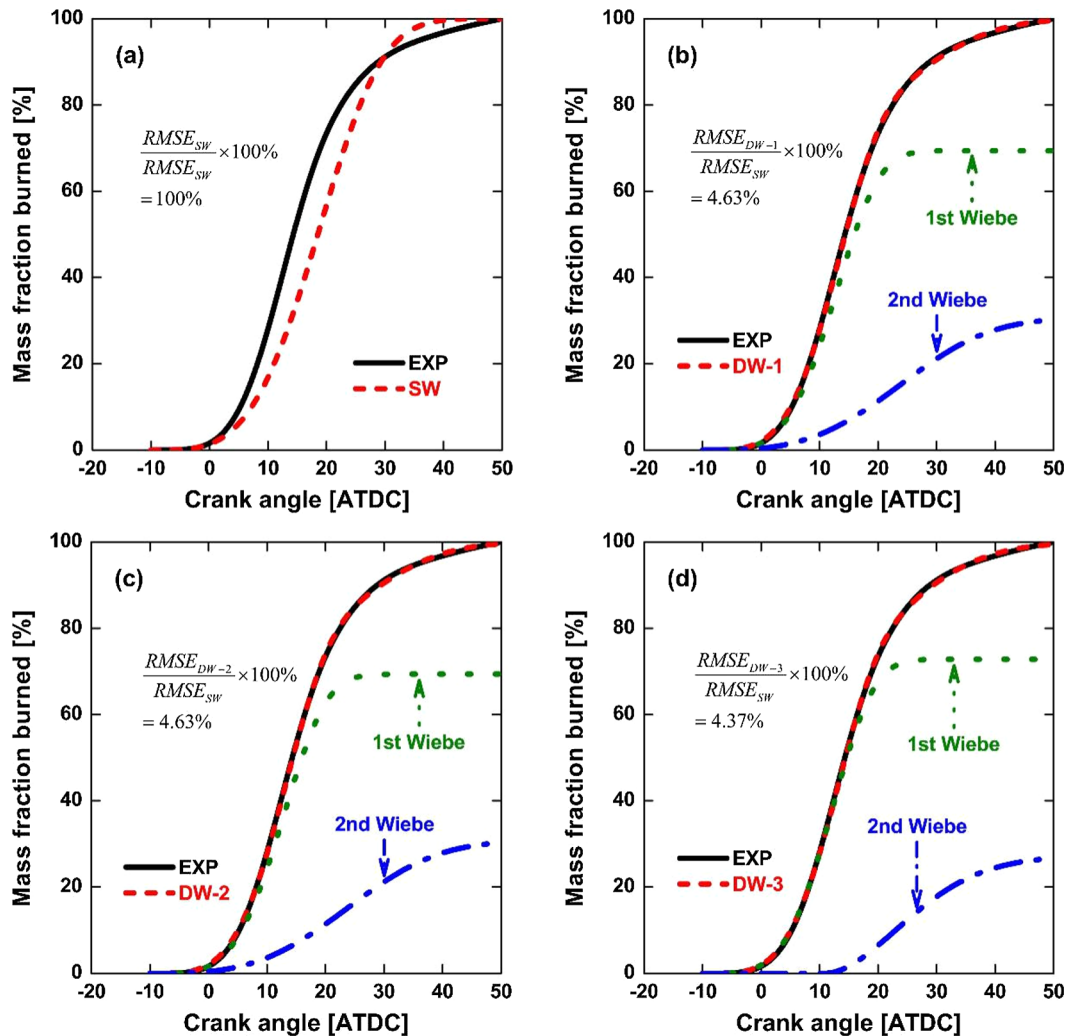


Fig. 4. Mass fraction burned predicted by the four Wiebe function formats compared to the experimental data: (a) standard Wiebe function, (b) double-Wiebe function - 1st format, (c) double-Wiebe function - 2nd format, and (d) double-Wiebe function - 3rd format.

Wiebe function for premixed SI combustion. The value of $m = 2.73$ in Eq. (12) meets this rule. A closer investigation of Eqs. (13) and (14) will reveal that their second Wiebe functions are identical. This is normal, as they had the same combined α factor (see Eq. (3)) even if the a_2 and $\Delta\theta_2$ were different and proves that the efficiency parameter and combustion duration for the second combustion stage were correlated. Again, the value of $m_2 = 2.22$ suggest a relatively symmetric burn in the second stage, which is probably different from the real process. For example, the 3D CFD simulation in Ref. [9] suggested that the second stage has a long tail in terms of rate of heat release. Moreover, while Eqs. (13) and (14) have a different m_1 in their first Wiebe function (m_1 equal to 2.41 and 3.18, respectively), which suggested that Eq. (13) predicted a faster initial burned during the first stage compared to Eq. (14), However, the percentages of fuel that burned in the first stage were similar (0.69). As the *RMSE* in Fig. 4b and c were similar, this suggests the limitation of using data at only one operating condition to determine the Wiebe-function parameters (Note: the reader is reminded that goal here was to compare the prediction performance of each Wiebe function format, not to find the appropriate model parameters that can be used for all the operating conditions of this NG SI engine). In addition, despite the 95% reduction in the *RSME* produced by the 1st and 2nd Wiebe-function formats compared the standard Wiebe function, there were still some minor differences compared to the experiment. For example, the higher MFB from ST to ~ 5 CAD ATDC and lower MFB from 25 to 35 CAD ATDC seen in Fig. 4b and c suggests that these double-Wiebe formats predicted a faster early flame development process. This was probably due to the assumption that both combustion stages started at the same time, which is different from the real phenomena. This is the main reason why the 3rd double-Wiebe format improved the prediction shown in Fig. 4d. Moreover, the *RSME* for the 3rd double-Wiebe model further reduced by a further 6% compared to the 1st or 2nd double-Wiebe formats. Furthermore, the 3rd double-Wiebe model predicted a higher percentage of fuel burned during the 1st combustion stage (72%), due to the delayed start of 2nd combustion stage. The form parameters in the 3rd Wiebe-function format predicted a burn rate that was closer to the real phenomena. For example, $m_1 = 3.19$ suggested that the first stage had a slower flame inception but faster flame propagation after, while $m_2 = 0.82$ suggested that the second stage had a fast-initial burn but slower late combustion. This is very similar to what was seen during the visualization of the combustion process in this engine [11]. This phenomenon can be explained by a relatively faster combustion at the entrance of the squish compared to much slowly burning deeply inside the squish for the conditions investigated here. Specifically, the squish entrance had a higher turbulence due to the reverse flow compared to the deeper region inside the squish, especially at a much later expansion stroke [11]. While Fig. 4 indicated that all the double-Wiebe formats predicted much better the MFB in NG SI premixed combustion inside diesel geometry compared to the standard Wiebe function, the results suggested that the 3rd format of double-Wiebe function should be used for more accurate MFB analysis in such retrofitted engines.

The effect of the form factor m is more evident in Fig. 5, which compared the predicted and experimental AHRR using the MFB data. Fig. 5a shows that the standard Wiebe function delayed the flame propagation, evidenced by the lower and retarded heat release peak. The three double-Wiebe-function formats performed much better, reducing the *RSME* by 88%. Similar to Fig. 4, Fig. 5b and c show a faster start of combustion due to the assumption that the slow-burn event started at spark timing. As a result, the double-Wiebe function slightly delayed the flame propagation process during the fully developed turbulent combustion process, evidenced by the delayed peak in the heat release. Moreover, Fig. 5b and c show that the form factor m produced a symmetrical second combustion stage, which is different from the real phenomena in Ref. [9]. The 3rd double-Wiebe format predicted the best the heat-release process, evidenced by the non-symmetrical second combustion stage. For example, the 3D CFD simulation in Ref. [11]

predicted that the second combustion stage will start at ~ 11 CAD ATDC, which is close to the value predicted by the double-Wiebe model in Fig. 5d. In addition, the location of the flame-front predicted by the 3D CFD simulation in Ref. [8] suggested that the burn inside the bowl completed between 20 and 25 CAD ATDC, which is close to the values predicted by all three double-Wiebe formats. As the 3rd double-Wiebe combustion model agreed well with the 3D CFD simulations, it suggest that this OD model can provide the MFB information for both the inside-and outside-the-bowl combustion events, including the overlap between the two combustion stages (which cannot be easily determined from the 3D simulations). Consequently, the 3rd double-Wiebe format can add more information and assist existing tools for optimizing engine operation.

Fig. 6 compares the predicted and experimental in-cylinder pressure. Again, the standard Wiebe format had difficulties in predicting in-cylinder pressure, with Fig. 6a showing a lower and retarded peak pressure due to the lower burning rate inside the bowl. While Fig. 6b and c show that the first two formats of the double-Wiebe function predicted well in-cylinder pressure (evidenced by the 94% reduction in *RSME*), the pressure was slightly higher than the experimental data between TDC and 8 CAD ATDC, due to the second combustion stage beginning at spark timing. Although not clearly seen in the figures, the 1st and 2nd format of the double-Wiebe functions slightly retarded the predicted peak pressure, due to the slightly delayed flame front propagation. Fig. 6d shows that not only the 3rd format of the double-Wiebe function predicted very well in-cylinder pressure, but also slightly increased the prediction accuracy compared to the 1st and 2nd double-Wiebe combustion models.

Combustion phasing influences both engine performance and emissions. The MFB_x shown in Fig. 7 was defined as the crank angle associated with x% mass fraction burned using the Wiebe function. MFB10 is usually associated with the end of the early flame development period, MFB50 is often correlated with efficiency and emissions, and MFB90 is generally associated to the end of the bulk burning. Fig. 7 shows that the standard Wiebe function delayed MFB10, due to the delayed flame propagation seen in Figs. 4a and 5a. Moreover, the standard Wiebe function also delayed MFB50 and MFB90, as the single-Wiebe needed to predict a slower burn inside the bowl but a faster burn inside the squish compared to the experimental data in order to reduce the total error. On the other hand, all the three formats of the double-Wiebe function slightly advanced MFB10 and delayed MFB50 and MFB90, but the differences between the prediction and experimental data were very small. In addition, all models exhibited less accuracy in predicting MFB90, probably due to the high gradient near EOC. However, the 3rd double-Wiebe format produced the smallest differences compared to the experimental data, which further supports its use for predicting the performance of diesel engines converted to lean-burn NG SI operation.

5. Discussion

While the Wiebe-function parameters were determined based on one operating condition (i.e., a condition-dependent approach), the results showed that the OD combustion model using the double-Wiebe function greatly improved the MFB predictions during each of the two premixed-combustion stages inside the diesel geometry, compared to the traditional single-Wiebe function. However, it is also important to note that such a condition-dependent model is limited to the operating conditions used for determining the model parameters. Therefore, while the double-Wiebe-function parameters may change with the operating condition and are (probably) engine-specific [15], data from a large number of operating conditions or CFD simulations can be used to find the unique set (or sets) of parameters that can minimize the error at most conditions. For example, the form factors and efficiency parameters of the double-Wiebe function that predicts the combustion stages inside a diesel engine retrofitted to NG SI can be determined if

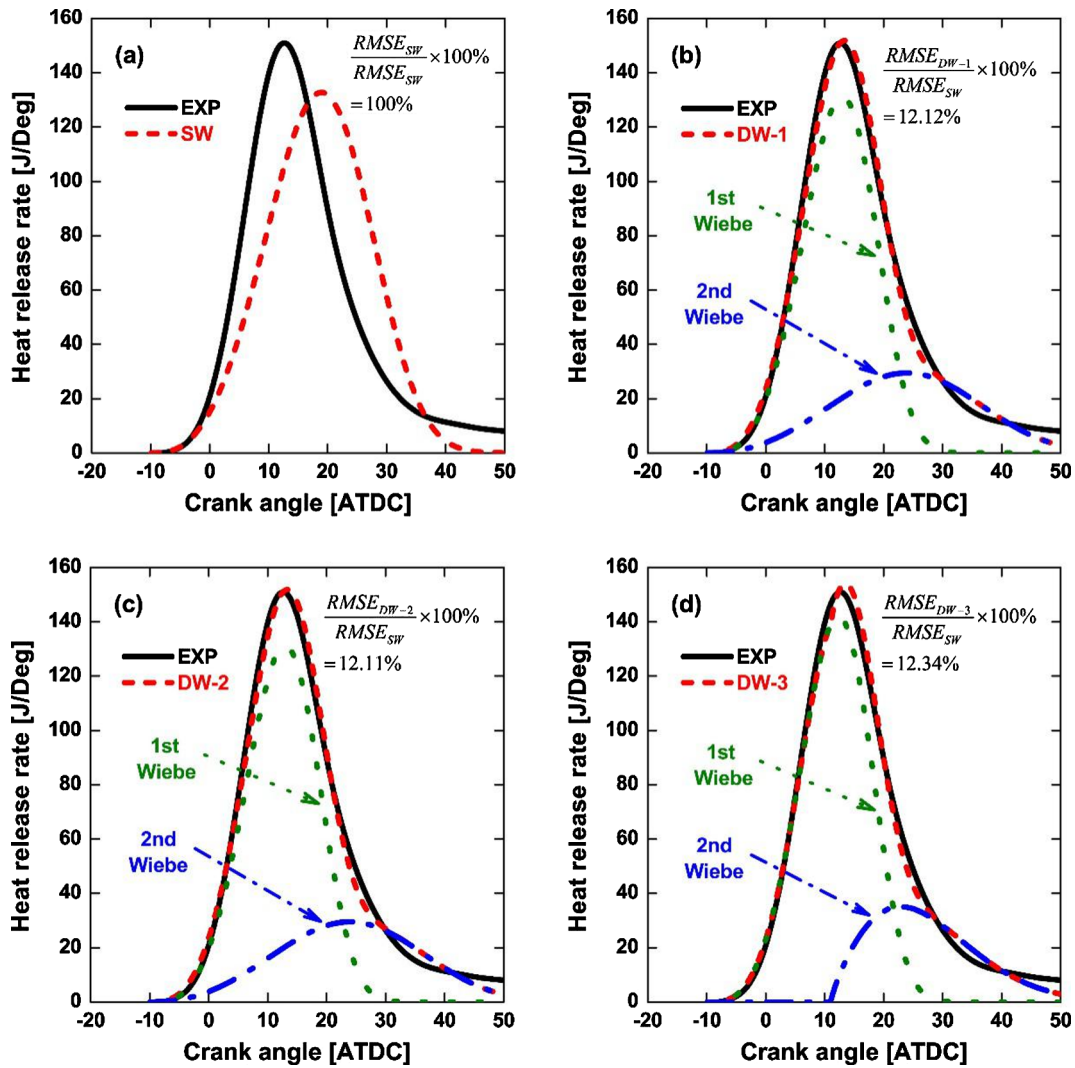


Fig. 5. Apparent heat release rate predicted by the four Wiebe function formats compared to the experimental data: (a) standard Wiebe function, (b) double-Wiebe function - 1st format, (c) double-Wiebe function - 2nd format, and (d) double-Wiebe function - 3rd format.

the dependence of λ , $\theta_{0,i}$, and $\Delta\theta_i$ on the operating conditions shown with Eqs. (17) and (18) is known:

$$\lambda = f(ST, \phi, N, T_{in}, P_{in}, EGR, etc.) \tag{17}$$

$$\theta_{0,i} = f(ST, \phi, N, T_{in}, P_{in}, EGR, etc.) \tag{18}$$

$$\Delta\theta_i = f(ST, \phi, N, T_{in}, P_{in}, EGR, etc.) \tag{19}$$

Eqs. (17)–(19) suggest that the methodology needs to know the effect of spark timing (ST), mixture equivalence ratio (ϕ), engine speed (N), intake temperature (T_{in}), intake pressure (P_{in}), exhaust gas recirculation (EGR), etc. on the start timing, the duration, and the mass fraction burned of each combustion stage. Consequently, 3D CFD tools or condition-dependent double-Wiebe model are needed to determine the λ , $\theta_{0,i}$, and $\Delta\theta_i$ for each operating condition. Then, a least-squares method can be applied to find the condition-independent Wiebe combustion model. Future work will focus on finding the condition-independent model for this particular engine.

6. Summary and conclusions

The addition of a high-energy spark plug to ignite the gas-air mixture and fumigating the gaseous fuel inside the intake manifold is an economical way to convert heavy-duty diesel engines to lean natural-gas spark-ignition operation. The use of simple but appropriate

combustion models to predict the combustion process in such retrofitted engines can accelerate and optimize the engine conversion. This study compared the standard single Wiebe function to a double-Wiebe function (i.e., 1st Wiebe function associated to the fast burn and the 2nd Wiebe function associated to the slower burn inside the squish) to investigate if the latter will improve the predicted mass fraction burned and, if yes, which of formats of the dual-Wiebe function in the literature described the best the mass fraction burned in such converted engine. The main findings were:

- A 0D combustion model using the standard Wiebe function could not predict the mass fraction burned in the two-stage combustion process characteristic of diesel engines converted to lean natural-gas spark-ignition operation because it was designed for a one-stage combustion process.
- A 0D combustion model using a double-Wiebe function (one for the fast burn inside the piston bowl and a second for the slower burning process inside the squish region) predicted with good accuracy the combustion process in such converted engines. Specifically, the double-Wiebe function predicted well the mass fraction burned, heat release rate, in-cylinder pressure, and combustion phasing.
- A format for the double-Wiebe function that delayed the start of the second combustion stage produced not only the best predictions, but they were also closer to the results obtained by detailed 3D CFD

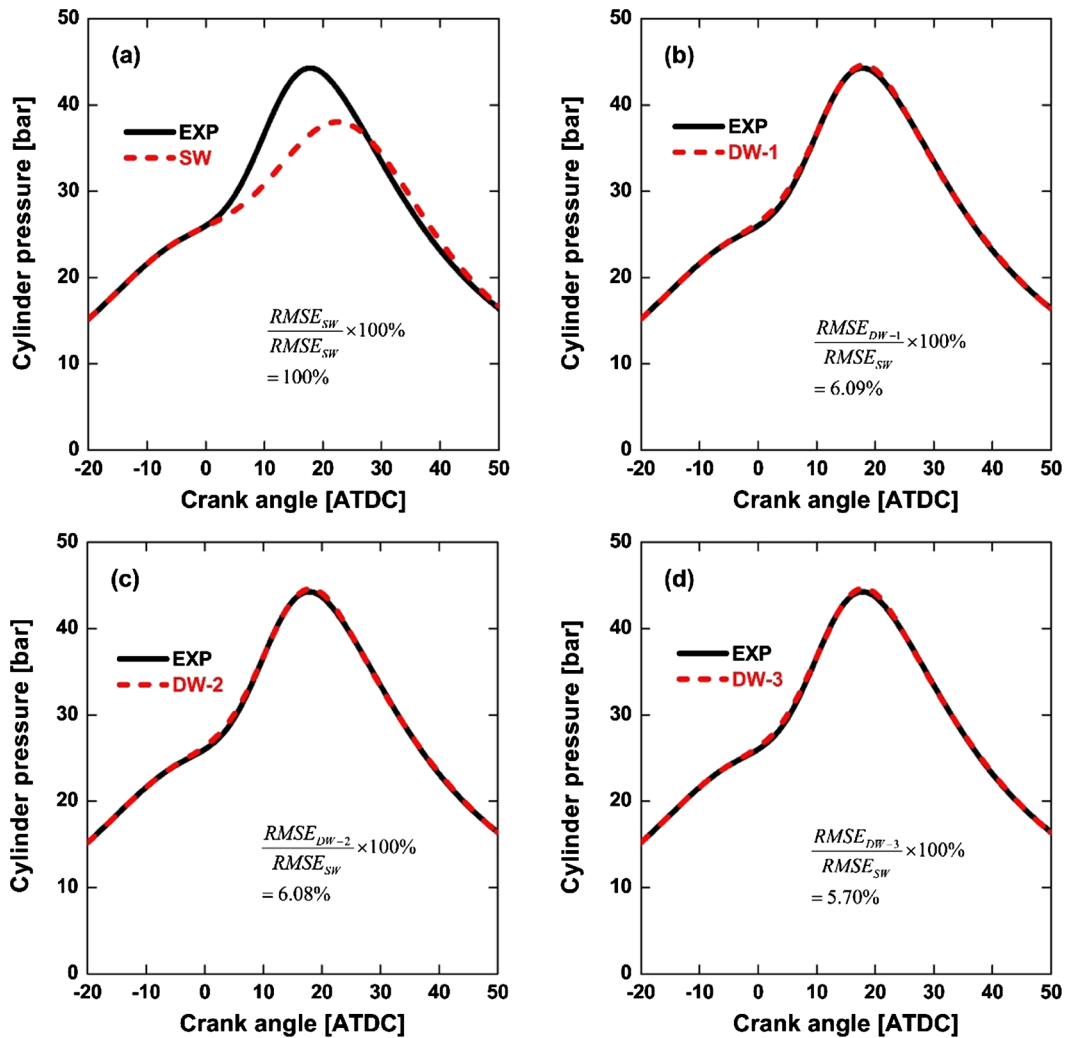


Fig. 6. Cylinder pressure predicted by the four Wiebe function formats compared to the experimental data: (a) standard Wiebe function, (b) double-Wiebe function - 1st format, (c) double-Wiebe function - 2nd format, and (d) double-Wiebe function - 3rd format.

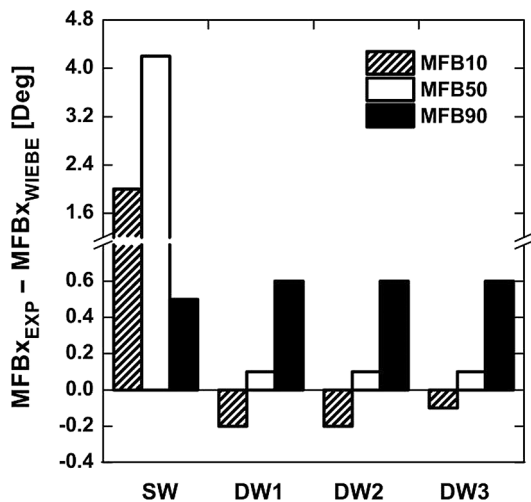


Fig. 7. Predicted and experimental combustion phasing (SW-single Wiebe, DW-double Wiebe).

simulations at the same operating conditions. As a result, the use of such model can accelerate the conversion of diesel engines to natural-gas spark-ignition operation.

- Such a condition-dependent model as the double-Wiebe model is

limited to the operating conditions used for determining the model parameters. However, the model can be developed into a condition-independent model if enough experimental data or CFD simulations are available to find that unique set (or sets) of parameters that minimizes the error at most conditions.

Acknowledgments

This research was conducted at the West Virginia University (WVU) Advanced Combustion Laboratory in Morgantown, WV. The material is based upon work funded by the WV Higher Education Policy Commission under grant number HEPC.dsr.18.7. The authors gratefully acknowledge WVU’s Center for Alternative Fuels Engines and Emissions (CAFEE), WVU’s Center for Innovation in Gas Research and Utilization (CIGRU), and the MAE department for their support and assistance with comprehensive mechanical, electronic, and data-acquisition hardware/software systems, respectively.

References

- [1] Bommisetty H, Liu J, Kooragayala R, Dumitrescu CE. Fuel composition effects in a CI engine converted to SI natural gas operation. SAE Technical Paper 2018-01-1137; 2018.
- [2] Stocchi I, Liu J, Dumitrescu CE, Battistoni M, Grimaldi CN. Effect of piston crevices on 3D simulation of a heavy-duty diesel engine retrofitted to natural gas spark ignition. ASME 2018 international mechanical engineering congress and exposition,

- November 9–15, 2018, Pittsburgh, PA, US. 2018.
- [3] Heywood JB. Internal combustion engine fundamentals. New York: McGraw-Hill; 1988.
- [4] Liu J. Gas investigation of combustion characteristics of a heavy-duty diesel engine retrofitted to natural gas spark ignition operation PhD. dissertation West Virginia University; 2018.
- [5] Johansson B, Olsson K. Combustion chambers for natural gas SI engines Part I: fluid flow and combustion. SAE Technical Paper 950469; 1995.
- [6] Liu J, Dumitrescu CE. CFD simulation of metal and optical configuration of a heavy-duty CI engine converted to SI natural gas. Part 2: in-cylinder flow and emissions. SAE Technical Paper 2019-01-0003; 2019.
- [7] Liu J, Dumitrescu CE. Numerical simulation of re-entrant bowl effects on natural gas SI operation. ASME 2018 internal combustion engine division fall technical conference, November 4–7, 2018, San Diego, CA, US. 2018.
- [8] Liu J, Dumitrescu CE. 3D CFD simulation of a CI engine converted to SI natural gas operation using the G-equation. Fuel 2018;232:833–44.
- [9] Liu J, Dumitrescu CE. Combustion partitioning inside a natural gas spark ignition engine with a bowl-in-piston geometry. Energy Convers Manage 2019;183:73–83.
- [10] Dumitrescu CE, Padmanaban V, Liu J. An experimental investigation of early flame development in an optical SI engine fueled with natural gas. J Eng Gas Turb Power 2018;140(8):082802.
- [11] Liu J, Dumitrescu CE. CFD simulation of metal and optical configuration of a heavy-duty CI engine converted to SI natural gas. Part 1: combustion behavior. SAE Technical Paper 2019-01-0002; 2019.
- [12] Liu J, Dumitrescu CE. Flame development analysis in a diesel optical engine converted to spark ignition natural gas operation. Appl Energy 2018;230:1205–17.
- [13] Liu J, Dumitrescu CE. Optical analysis of flame inception and propagation in a lean-burn natural-gas spark-ignition engine with a bowl-in-piston geometry. Int J Engine Res 2019. 1468087418822852.
- [14] Liu J, Dumitrescu CE. Lean-burn characteristics of a heavy-duty diesel engine retrofitted to natural gas spark ignition. J Eng Gas Turb Power 2019;141(7):071013.
- [15] Yasar H, Soyhan HS, Walmsley H, Head B, Sorusbay C. Double-Wiebe function: an approach for single-zone HCCI engine modeling. Appl Therm Eng 2008;28:1284–90.
- [16] Yeliana Y, Cooney C, Worm J, Michalek DJ, Naber JD. Estimation of double-Wiebe function parameters using least square method for burn durations of ethanol-gasoline blends in spark ignition engine over variable compression ratios and EGR levels. Appl Therm Eng 2011;31:2213–20.
- [17] Heywood J. Engine combustion modeling-an overview. Combustion modeling in reciprocating engines; 1980.p. 1–35.
- [18] Glewen WJ, Wagner RM, Edwards KD, Daw CS. Analysis of cyclic variability in spark-assisted HCCI combustion using a double Wiebe function. Proc Combust Inst 2009;32:2885–92.
- [19] Tolou S, Vedula RT, Schock H, Zhu G, Sun Y, Kotrba A. Combustion model for a homogeneous turbocharged gasoline direct-injection engine. J Eng Gas Turb Power 2018;140:102804–10.
- [20] Awad S, Varuvel EG, Loubar K, Tazerout M. Single zone combustion modeling of biodiesel from wastes in diesel engine. Fuel 2013;106:558–68.
- [21] Xu S, Anderson D, Singh A, Hoffman M, Prucka R, Filipi Z. Development of a phenomenological dual-fuel natural gas diesel engine simulation and its use for analysis of transient operations. SAE Int J Engines 2014;7:1665–73.
- [22] Xu S, Anderson D, Hoffman M, Prucka R, Filipi Z. A phenomenological combustion analysis of a dual-fuel natural-gas diesel engine. Proc Inst Mech Eng Part D: J Automob Eng 2016;231:66–83.
- [23] Caligiuri C, Renzi M. Combustion modelling of a dual fuel diesel - producer gas compression ignition engine. Energy Proc 2017;142:1395–400.
- [24] Larmi M, Isaksson S, Tikkanen S, Lammila M. Performance simulation of a compression ignition free piston engine. SAE Technical Paper 2001-01-0280; 2001.
- [25] Liu J, Bommisetty H, Dumitrescu CE. Experimental investigation of a heavy-duty CI engine retrofitted to natural gas SI operation. ASME ICEF2018 internal combustion engine division fall technical conference, November 4–7, 2018, San Diego, CA, US. 2018.
- [26] Cooney C, Worm J, Michalek D, Naber J. Wiebe function parameter determination for mass fraction burn calculation in an ethanol-gasoline fuelled SI engine. J KONES 2008;15:567–74.
- [27] Woschni, G. A universally applicable equation for the instantaneous heat transfer coefficient in the internal combustion engine. SAE Technical Paper 670931; 1967.